Combination of Noncovalent Mass Spectrometry and Traveling Wave Ion Mobility Spectrometry Reveals Sugar-Induced Conformational Changes of Central Glycolytic Genes Repressor/DNA Com...

ARTICLE *in* ANALYTICAL CHEMISTRY · APRIL 2010

Impact Factor: 5.64 · DOI: 10.1021/ac902784n · Source: PubMed

Anal. Chem. **2010,** *82,* 3597–3605

Combination of Noncovalent Mass Spectrometry and Traveling Wave Ion Mobility Spectrometry Reveals Sugar-Induced Conformational Changes of Central Glycolytic Genes Repressor/DNA Complex

Cédric Atmanene,[†] Denix Chaix,[‡] Yannick Bessin,[‡] Nathalie Declerck,[‡] Alain Van Dorsselaer,[†] and Sarah Sanglier-Cianferani*[,†]

Laboratoire de Spectrométrie de Masse BioOrganique, Université de Strasbourg, IPHC, 25 rue Becquerel, 67087 STRASBOURG, France, CNRS UMR7178, 67087 Strasbourg, France and INSERM U554, Centre de Biochimie Structurale, CNRS UMR5048 and Université Montpellier 1, 29 rue de Navacelles, F-34090 Montpellier, France

The central glycolytic genes repressor (CggR) is a 37 kDa transcriptional repressor protein which plays a key role in *Bacillus subtilis* glycolysis by regulating the transcription of the *gapA* operon. Fructose-1,6-bisphosphate (FBP), identified as the effector sugar, has been shown to abolish the binding cooperativity of CggR to its DNA target and to modify the conformational dynamics of the CggR/DNA complex. In the present study, noncovalent mass spectrometry (MS) was used to obtain deeper insights into FBP-dependent CggR/DNA interactions. The effect of FBP binding on CggR alone and on CggR/DNA complexes was examined using automated chip-based nanoelectrospray MS and traveling wave ion mobility mass spectrometry (IM-MS). Our results revealed that tetrameric CggR dissociates into dimers upon FBP binding. Moreover, FBP binding to CggR/DNA complexes triggers disruption of intermolecular protein/protein interactions within the complex, significantly modifying its conformation as evidenced by a 5% increase of its collision cross section. For the first time, the use of IM-MS is reported to probe ligand-induced conformational modifications of a protein/DNA complex with an emphasis on the comparison with solution-based techniques.

The central glycolytic genes repressor (CggR) is a 37 kDa transcriptional repressor protein which plays a key role in *Bacillus subtilis* glycolysis by regulating the transcription of the *gapA* operon.[1−3] While CggR is encoded by the first gene of this hexacistronic operon, key glycolytic enzymes are the products of five additional genes.[4,5] CggR acts as a transcriptional repressor of the *gapA* operon by binding to a DNA operator sequence located in the *cggR* gene leader region.[6] The full-length operator consists of a 45-basepair DNA sequence containing two direct repeats.[6] Interactions between CggR and both the full-length operator (O_{LR}) as well as the independent left (O_L) and right (O_R) half-site operators have been extensively studied using several biophysical techniques.[6–9] These investigations revealed that CggR binds to its full-length target DNA as a tetramer. CggR can also bind to each individual half-site operator as a dimer with a better affinity for O_R.[7,9] Moreover, the oligomerization state of CggR and its interaction with DNA have been shown to be modulated by the binding of fructose-1,6-bisphospate (FBP).[6,7,9] FBP has a dual role on CggR: at low concentration, it acts as a cofactor that stabilizes the protein and favors the formation of dimers over higher order oligomers; at high concentration, it modifies the binding cooperativity of CggR to its DNA target and, thereby, reduces the affinity of the tetrameric CggR/DNA complex.[7,9,10] These observations have been interpreted as arising from disruption of intermolecular protein/protein interactions, leading to the dissociation of CggR tetramer in two independent dimers which remain bound to the DNA sequence, preserving thus the 4:1 CggR/DNA binding stoichiometry.[9]

Deciphering the intricate biological mechanisms involved in the regulation of gene expression is a challenging task, which often requires complementary approaches combining the benefits of orthogonal biophysical techniques to study protein/DNA interactions. In this context, nanoelectrospray mass spectrometry (nanoESI-MS) plays a key role as demonstrated by the growing number of reported

* Corresponding author. Phone: +33 (0)3 68 85 26 79. Fax: +33 (0)3 68 85 27 81. E-mail: sarah.cianferani@unistra.fr.

[†] Université de Strasbourg.

[‡] CNRS (UMR5048) and Université Montpellier 1.

(1) Fillinger, S.; Boschi-Muller, S.; Azza, S.; Dervyn, E.; Branlant, G.; Aymerich, S. *J. Biol. Chem.* **2000**, *275*, 14031–14037.

(2) Ludwig, H.; Homuth, G.; Schmalisch, M.; Dyka, F. M.; Hecker, M.; Stulke, J. *Mol. Microbiol.* **2001**, *41*, 409–422.

(3) Fuhrer, T.; Fischer, E.; Sauer, U. *J. Bacteriol.* **2005**, *187*, 1581–1590.

(4) Kunst, F.; Ogasawara, N.; Moszer, I.; Albertini, A. M.; Alloni, G.; Azevedo, V.; Bertero, M. G.; Bessieres, P.; Bolotin, A.; Borchert, S.; Borriss, R.; Boursier, L.; Brans, A.; Braun, M.; Brignell, S. C.; Bron, S.; Brouillet, S.; Bruschi, C. V.; Caldwell, B.; Capuano, V.; Carter, N. M.; Choi, S. K.; Codani, J. J.; Connerton, I. F.; Danchin, A.; et al. *Nature* **1997**, *390*, 249–256.

(5) Tobisch, S.; Zuhlke, D.; Bernhardt, J.; Stulke, J.; Hecker, M. *J. Bacteriol.* **1999**, *181*, 6996–7004.

(6) Doan, T.; Aymerich, S. *Mol. Microbiol.* **2003**, *47*, 1709–1721.

(7) Zorrilla, S.; Chaix, D.; Ortega, A.; Alfonso, C.; Doan, T.; Margeat, E.; Rivas, G.; Aymerich, S.; Declerck, N.; Royer, C. A. *Biochemistry* **2007**, *46*, 14996–15008.

(8) Doan, T.; Martin, L.; Zorrilla, S.; Chaix, D.; Aymerich, S.; Labesse, G.; Declerck, N. *Proteins* **2008**, *71*, 2038–2050.

(9) Zorrilla, S.; Doan, T.; Alfonso, C.; Margeat, E.; Ortega, A.; Rivas, G.; Aymerich, S.; Royer, C. A.; Declerck, N. *Biophys. J.* **2007**, *92*, 3215–3227.

(10) Rezacova, P.; Kozisek, M.; Moy, S. F.; Sieglova, I.; Joachimiak, A.; Machius, M.; Otwinowski, Z. *Mol. Microbiol.* **2008**, *69*, 895–910.

10.1021/ac902784n
Published on Web 04/02/2010

works focused on the characterization of protein/oligonucleotide complexes.[11−21] Since the first demonstrations of the possibility to analyze intact noncovalent assemblies in the gas phase using electrospray ionization,[22,23] important methodological and instrumental achievements have been made, allowing complexes of various compositions and different sizes ranging from several hundred up to several million Daltons to be investigated with this technique.[24] On the basis of accurate mass measurements, noncovalent MS (i.e., MS for the study of noncovalent assemblies) can provide crucial information on protein oligomerization states and protein/ligand binding stoichiometries.[25−27] Moreover, MS-based strategies have also been developed to provide insights into the 3D architecture of intact proteins and noncovalent complexes. These strategies include charge state distribution analysis,[28−30] limited proteolysis,[31−33] and footprinting techniques (e.g., H/D exchange[28−30] or hydroxyl radical labeling[30,34,35]), as well as chemical and gas-phase dissociation of intact complexes,[14,25,36] which altogether provide information on topology, solvent-exposed area, interaction networks, and conformational dynamics of supramolecular assemblies.

More recently, traveling wave ion mobility mass spectrometry (IM-MS) has been introduced as a powerful technique to probe the size/shape of macromolecular ions in the gas phase.[24,37−43] The basic principle of IM-MS relies on the ability of gas-phase ions to fly through a neutral buffer gas under the influence of a weak electric field. Ions with extended structure experience more collisions with the buffer gas than ions with compact structure. Since those collisions impede ion progression through the ion mobility cell, information on the shape/size of gas-phase ions can be derived from the measurement of their drift time, i.e., the time required by an ion to traverse the ion mobility cell.

In the present work, we used a combination of MS-based techniques to investigate FBP-modulated interactions between CggR and its target DNA. As a first step, automated chip-based nanoESI-MS experiments were carried out in nondenaturing conditions to investigate the effect of FBP binding on both CggR oligomerization state and CggR/DNA complex stability. Using a protein/DNA assembly formed with two DNA binding sites (half-site operators) on separate oligonucleotides, we demonstrated that FBP-binding disrupts protein/protein interactions within CggR/DNA complex. The impact of such structural modifications on the CggR/full-length DNA complex was subsequently investigated using nanoESI-IM-MS, which revealed significant conformational changes triggered upon sugar binding. Finally, data provided by nanoESI-IM-MS experiments are discussed in light of the results obtained by size-exclusion chromatography (SEC) and small-angle X-ray scattering (SAXS), highlighting both the qualitative and quantitative correlation between gas-phase nanoESI-IM-MS measurements and data from solution-based techniques.

EXPERIMENTAL SECTION

Protein Expression and Purification. CggR was produced in *E. coli* with a N-terminal His-tag and the protein was purified by affinity chromatography as described previously.[6,9] Cells were resuspended in 50 mM Tris−HCl, 150 mM NaCl, 10 mM imidazole, 3 mM β-mercaptoethanol, 1 mM benzamidine, and pH 8 buffer (HT buffer) supplemented with 5 mM benzamidine. Cells were lysed by sonication after a 30 min incubation on ice with 0.2 mg/mL lysozyme together with 2 μg/mL DNase 1 and 50 mM Na_2HPO_4. After centrifugation at 18 000 rpm for 20 min at 4 C, the cell supernatant was loaded onto a Ni^{2+}-NTA agarose resin (Qiagen, Germantown, MD) and incubated for 30 min at 4 C with gentle shaking. The resin was then washed extensively with HT buffer supplemented with, successively, 0.125% glycerol and 50 mM Na_2HPO_4, 1 M NaCl, 0.4 M KCl, and 20 mM imidazole, before eluting the protein with a 300 mM imidazole in HT buffer. The most concentrated fractions were dialyzed against 20 mM Tris−HCl, 150 mM NaCl, 2 mM DTT, and 2 mM EDTA, 10% glycerol buffer, pH 8. The fractions were pooled and protein aliquots were stored at −80 C. Protein concentration was determined by the Bradford assay.

Protein/DNA Complexes Purification. The oligonucleotides containing the full-length O_{LR} operator (45 bp 5′-TGACGGGACGTTTTTTGTCATAGCGGGACATATAATGTCCAGCAA-3′) or the half-site O_R (23 bp 5′-TAGCGGGACATATAATGTCCAGC-3′) were purchased from Eurogentec. The sense and

(11) Ritschel, T.; Atmanene, C.; Reuter, K.; Van Dorsselaer, A.; Sanglier-Cianferani, S.; Klebe, G. *J. Mol. Biol.* **2009**, *393*, 833–847.
(12) Kilic, T.; Sanglier, S.; Van Dorsselaer, A.; Suck, D. *Protein Sci.* **2006**, *15*, 2310–2317.
(13) Kurimoto, K.; Kuwasako, K.; Sandercock, A. M.; Unzai, S.; Robinson, C. V.; Muto, Y.; Yokoyama, S. *Proteins* **2009**, *75*, 360–372.
(14) Gordiyenko, Y.; Robinson, C. V. *Biochem. Soc. Trans.* **2008**, *36*, 723–731.
(15) Barraud, P.; Golinelli-Pimpaneau, B.; Atmanene, C.; Sanglier, S.; Van Dorsselaer, A.; Droogmans, L.; Dardel, F.; Tisne, C. *J. Mol. Biol.* **2008**, *377*, 535–550.
(16) Turner, K. B.; Hagan, N. A.; Fabris, D. *J. Mol. Biol.* **2007**, *369*, 812–828.
(17) Hagan, N. A.; Fabris, D. *J. Mol. Biol.* **2007**, *365*, 396–410.
(18) Hanson, C. L.; Robinson, C. V. *J. Biol. Chem.* **2004**, *279*, 24907–24910.
(19) Rusconi, F.; Guillonneau, F.; Praseuth, D. *Mass Spectrom. Rev.* **2002**, *21*, 305–348.
(20) Hofstadler, S. A.; Griffey, R. H. *Chem. Rev.* **2001**, *101*, 377–390.
(21) Beck, J. L.; Colgrave, M. L.; Ralph, S. F.; Sheil, M. M. *Mass Spectrom. Rev.* **2001**, *20*, 61–87.
(22) Ganem, B.; Li, Y. T.; Henion, J. D. *J. Am. Chem. Soc.* **1991**, *113*, 6294–6296.
(23) Katta, V.; Chait, B. T. *J. Am. Chem. Soc.* **1991**, *113*, 8534–8535.
(24) Uetrecht, C.; Versluis, C.; Watts, N. R.; Wingfield, P. T.; Steven, A. C.; Heck, A. J. *Angew. Chem., Int. Ed. Engl.* **2008**, *47*, 6247–6251.
(25) Heck, A. J. *Nat. Methods* **2008**, *5*, 927–933.
(26) Hernandez, H.; Robinson, C. V. *Nat. Protoc.* **2007**, *2*, 715–726.
(27) Sanglier, S.; Atmanene, C.; Chevreux, G.; Van Dorsselaer, A. *Methods Mol. Biol.* **2008**, *484*, 217–243.
(28) Kaltashov, I. A.; Eyles, S. J. *Mass Spectrom. Rev.* **2002**, *21*, 37–71.
(29) Eyles, S. J.; Kaltashov, I. A. *Methods* **2004**, *34*, 88–99.
(30) Konermann, L.; Tong, X.; Pan, Y. *J. Mass Spectrom.* **2008**, *43*, 1021–1036.
(31) Shields, S. J.; Oyeyemi, O.; Lightstone, F. C.; Balhorn, R. *J. Am. Soc. Mass Spectrom.* **2003**, *14*, 460–470.
(32) Hager-Braun, C.; Tomer, K. B. *Expert Rev. Proteomics* **2005**, *2*, 745–756.
(33) Downard, K. M. *Proteomics* **2006**, *6*, 5374–5384.
(34) Maleknia, S. D.; Downard, K. *Mass Spectrom. Rev.* **2001**, *20*, 388–401.
(35) Takamoto, K.; Chance, M. R. *Annu. Rev. Biophys. Biomol. Struct.* **2006**, *35*, 251–276.
(36) Sharon, M.; Mao, H.; Boeri Erba, E.; Stephens, E.; Zheng, N.; Robinson, C. V. *Structure* **2009**, *17*, 31–40.
(37) Ruotolo, B. T.; Giles, K.; Campuzano, I.; Sandercock, A. M.; Bateman, R. H.; Robinson, C. V. *Science* **2005**, *310*, 1658–1661.
(38) Ruotolo, B. T.; Benesch, J. L. P.; Sandercock, A. M.; Hyung, S.; Robinson, C. V. *Nat. Protoc.* **2008**, *3*, 1139–1152.
(39) Lorenzen, K.; Olia, A. S.; Uetrecht, C.; Cingolani, G.; Heck, A. J. *J. Mol. Biol.* **2008**, *379*, 385–396.
(40) Scarff, C. A.; Thalassinos, K.; Hilton, G. R.; Scrivens, J. H. *Rapid Commun. Mass Spectrom.* **2008**, *22*, 3297–3304.
(41) Smith, D. P.; Knapman, T. W.; Campuzano, I.; Malham, R. W.; Berryman, J. T.; Radforda, S. E.; Ashcroft, A. E. *Eur. J. Mass Spectrom.* **2009**, *15*, 113–130.
(42) Duijn, E.; Barendregt, A.; Synowsky, S.; Versluis, C.; Heck, A. J. *J. Am. Chem. Soc.* **2009**, *131*, 1452–1459.
(43) Scarff, C. A.; Patel, V. J.; Thalassinos, K.; Scrivens, J. H. *J. Am. Soc. Mass Spectrom.* **2009**, *20*, 625–631.

antisense strands were hybridized by heating a mixture at 50 μM in TE buffer and 150 mM NaCl to 90 C for 10 min and slowly cooling down to room temperature using a thermocycler. Complexes with DNA were formed by mixing the purified protein and DNA at a molar ratio of 4:1 (O_{LR}) or 2:1 (O_R) (protein/DNA) in a final volume of 500 μL. The complex was purified by size exclusion chromatography, using a Superdex 200 HR 10/30 (GE Healthcare) column pre-equilibrated with 20 mM Tris−HCl, pH 8.0, containing 150 mM NaCl, 2 mM EDTA, and 2 mM DTT. Protein/DNA complexes were eluted in a single peak, and the most concentrated fractions (500 μL) were pooled and eventually concentrated to a final protein concentration of 1 mg/mL as estimated by the Bradford assay.

Sample Buffer Exchange. Prior to any mass spectrometry experiments, CggR and CggR/DNA complexes were desalted against 150 mM ammonium acetate solution (pH 8.0, adjusted with ammonia). While CggR was buffer exchanged using a microcentrifuge gel filtration column (Zeba 0.5 mL, Thermo Scientific, Rockford, IL), CggR/DNA complexes were buffer exchanged using seven successive concentration/dilution steps performed with centrifugal concentrators (Vivaspin, 30 kDa molecular-weight cutoff membranes, Sartorius, Göttingen, Germany). Protein concentration was determined by the Bradford assay. Fructose-1,6-bisphosphate (FBP) trisodium salt hydrate was purchased from Sigma Aldrich (Steinheim, Germany), and sodium counterions were exchanged against volatile ammonium ions using a 1 mL anionic exchange column (HiTrap Q-Sepharose, GE Healthcare, Little Chalfont, UK). Subsequent quantification of desalted FBP was performed by LC-MS/MS analysis using an HPLC system (1100 Series, Agilent Technologies, Santa Clara, CA) coupled to an electrospray triple quadrupole mass spectrometer (LC/MS 6410B, Agilent Technologies, Santa Clara, CA).

Noncovalent NanoESI-MS Experiments. Noncovalent mass spectrometry experiments were carried out on an electrospray time-of-flight mass spectrometer (LCT, Waters, Manchester, UK) equipped with an automated chip-based nanoelectrospray source (Triversa Nanomate, Advion Biosciences, Ithaca, NY). Mass spectra were recorded in the positive ion mode over the mass range m/z 500−12000 after calibration with a 2 mg/mL solution of cesium iodide in 2-propanol/water (1/1). His-tagged CggR monomer molecular weight was first measured in denaturing conditions by diluting the protein to 5 μM in a 1:1 (v/v) water/acetonitrile mixture acidified with 1% (v/v) formic acid. Measured molecular weight (38780.3 ± 0.8 Da) was in good agreement with the mass calculated from the theoretical amino acid sequence (38780.8 Da). Experiments under nondenaturing conditions were performed by diluting samples in 150 mM ammonium acetate buffer, pH 8.0. Instrumental settings were carefully tuned in order to preserve the integrity of noncovalent assemblies in the gas phase while ensuring an optimal ion desolvation and transmission through the mass spectrometer. This optimization especially concerns the pressure (Pi) in the first pumping stage of the instrument as well as the accelerating voltage applied on the sampling cone (Vc). Vc and Pi values were adjusted differently for CggR and CggR/DNA assemblies and were reported in the figures legends. Data analysis was performed with MassLynx 4.1 (Waters, Manchester, UK).

Traveling Wave Ion Mobility Mass Spectrometry (IM-MS). *Instrumental Settings.* NanoESI-IM-MS experiments were performed using a hybrid quadrupole/ion mobility separator/time-of-flight instrument (Synapt HDMS, Waters, Manchester, UK) described elsewhere.[44] External calibration was performed in the positive ion mode with a 3 mg/mL solution of cesium iodide in 2-propanol/water (1/1). Samples were infused using 4 μm i.d. PicoTip nanospray emitters (New Objective, Woburn, MA), and ion mobility data were recorded after careful optimization of instrumental parameters (see Supporting Information, S1). Particularly, while the pressure in the first pumping stage (backing pressure) and in the Trap T-wave device were raised to 5.1 mbar and 0.065 mbar, respectively, the accelerating voltage applied on the sampling cone, the trap collision energy voltage (Trap CE), and the trap bias voltage were set to 50, 10, and 15 V, respectively. For mobility separation, the wave height, the wave velocity, and the nitrogen pressure in the ion mobility cell were, respectively, set to 11 V, 300 m/s, and 0.5 mbar corresponding to optimized parameters providing an improved separation of ions displaying different mobilities. Additional details are given in Supporting Information, S1.

Estimation of Theoretical and Experimental Collision Cross Section (CCS). Theoretical CCS were determined using the open source program MOBCAL,[45,46] which was modified as described elsewhere.[38] Coordinate files for free and FBP-bound CggR/O_{LR} complex were obtained from SAXS data modeling using the program SASREF.[47] Only CCS calculated with the exact hard sphere scattering (EHSS) method are reported here since it provides better CCS estimations for proteins than the projection approximation model does, and it requires much less computation time compared to the trajectory method.[40,43,48]

Regarding experimental CCS estimation, several studies have reported the use of ions with known collision cross section (CCS) to obtain an empirical relationship allowing the CCS of an analyte of interest to be derived from its mass- and charge-corrected drift time as measured by traveling wave IM-MS experiments.[24,37–43] Indeed, denatured proteins are generally used to calibrate the instrument for the determination of CCS between 1000 and 4000 Å^2, which corresponds approximately to spherical proteins between 10 and 70 kDa.[38] In the present study, complexes of interest display molecular weights of about 185 kDa, requiring a long extrapolation of the calibration curve to assess their CCS. As a consequence, denatured bovine ubiquitin and equine cytochrome C as well as horse heart myoglobin were used to create a calibration curve defined with a maximum number of points as previously described by Ruotolo et al.[38] This curve was subsequently used to assess the CCS of bovine liver catalase in nondenaturing conditions. This protein forms a large tetrameric assembly of about 236 kDa, and its CCS can be

(44) Pringle, S. D.; Giles, K.; Wildgoose, J. L.; Williams, J. P.; Slade, S. E.; Thalassinos, K.; Bateman, R. H.; Bowers, M. T.; Scrivens, J. H. *Int. J. Mass Spectrom.* **2007**, *261*, 1–12.
(45) Shvartsburg, A. A.; Jarrold, M. F. *Chem. Phys. Lett.* **1996**, *261*, 86–91.
(46) Mesleh, M. F.; Hunter, J. M.; Shvartsburg, A. A.; Schatz, G. C.; Jarrold, M. F. *J. Phys. Chem.* **1996**, *100*, 16082–16086.
(47) Chaix, D.; Ferguson, M. L.; Atmanene, C.; Van Dorsselaer, A.; Sanglier-Cianferani, S.; Royer, C. A.; Declerck, N. *Nucleic Acids Res.*, in press.
(48) Jarrold, M. F. *Acc. Chem. Res.* **1999**, *32*, 360–367.

derived from its crystallographic structure (PDB file 1TGU),[49] providing thus a reference value to estimate the validity of this extrapolation. In the present work, the mean CCS of bovine liver catalase averaged over its five most intense charge states (+32 to +36) was 10 000 ± 350 Å^2, which was found to be in good agreement with the value of 9950 Å^2 calculated from its crystallographic structure using the EHSS method, and showed, thus, that reliable CCS estimations could be obtained from the extrapolation of the calibration curve up to 10 000 Å^2. CCS determination was performed in duplicate showing reproducibility better than 2%. Data analysis was performed with MassLynx 4.1 (Waters, Manchester, UK).

RESULTS AND DISCUSSION

NanoESI-MS Investigation of FBP-Binding Effect on CggR and CggR/DNA Complexes. *FBP-Binding Alters CggR Quaternary Structure.* In the present study, CggR was first analyzed alone in order to investigate its oligomerization state under the present experimental conditions. When diluted to 20 μM (monomer concentration), CggR is mainly detected as a tetramer (155145 ± 3 Da) accompanied to a lower extent by the monomeric (38781 ± 2 Da) and dimeric (77567 ± 3 Da) forms of the protein (Figure 1a). Experiments carried out with protein diluted from 10 to 40 μM showed no significant differences in this concentration range (data not shown).

The binding of FBP (340.1 Da), the inducer sugar of CggR, has been studied previously using a variety of techniques, providing insights into its binding stoichiometry and affinity, as well as its effect on protein structure and oligomerization state.[7,9,10] While these studies unequivocally showed that FBP binding prevents the formation of CggR high molecular weight aggregates, different sugar binding stoichiometries were proposed. Indeed, X-ray crystallography and isothermal titration calorimetry only detected a single FBP molecule bound per CggR monomer,[7,10] whereas fluorescence anisotropy, limited proteolysis, and pressure perturbation experiments suggested the presence of two nonequivalent FBP binding sites per CggR monomer.[7]

In the present study, the relative high mass resolution provided by the used technique allows a direct visualization of all different species present in solution, enabling thus to simultaneously observe FBP-binding effect on the CggR oligomerization state and to determine its binding stoichiometry to the protein. Titration experiments involving a fixed CggR concentration and increasing amounts of FBP were, thus, monitored by nanoESI-MS. NanoESI mass spectra obtained after incubation of CggR (20 μM) with 0.5 to 1.5 molar equivalents of FBP (10−30 μM) show that CggR tetramer is progressively dissociated into dimers, demonstrating that binding of this effector sugar triggers the disruption of intermolecular protein/protein interactions (Figure 1b−d).

Regarding FBP binding stoichiometry, the presence of an equimolar concentration of FBP (20 μM, Figure 1c) mainly leads to the binding of one sugar molecule per protein monomer. Interestingly, in the presence of 30 μM of FBP, the CggR tetramer is almost totally dissociated and the binding of a second FBP molecule per protein subunit is observed on the CggR monomer (1:2 CggR/FBP complex) and dimer (2:4 CggR/FBP complex). Unfortunately, attempts to saturate this second binding site failed because higher FBP concentrations decreased the signal-to-noise ratio of the mass spectra. Thus, to confirm the specificity of FBP binding, a negative control experiment was performed with fructose-1-phosphate (F1P) which displays no effect on the DNA binding activity of CggR.[8] NanoESI mass spectrum acquired under strictly identical experimental and instrumental conditions first shows that F1P does not trigger the dissociation of CggR tetramer (Figure 1e), confirming the specific role of FBP in the modulation of CggR quaternary structure. Moreover, no F1P binding is observed on CggR monomer and dimer. The fact that nanoESI mass spectra reflect subtle modifications of the ligand structure strongly suggests that complexes detected in the gas phase arise from a specific association in solution[50] and strengthens previous observations indicating the presence of a second FBP binding site per CggR subunit.[7,8] It is finally noteworthy that, whatever the FBP concentration, no $(CggR)_4(FBP)_n$ complexes could be detected. This observation suggests that CggR tetramer dissociates into dimers within the 2 min incubation period. However, it is not possible to infer from these results whether the binding of a single FBP molecule is sufficient to trigger this tetramer-to-dimer transition or if more than one FBP molecule per tetramer is necessary.

In conclusion, the present titration experiments highlight that FBP binding to CggR is responsible for the disruption of intermolecular protein/protein interactions leading to the dissociation of CggR tetramer into dimers. These results also corroborate the presence of two FBP binding sites per CggR subunit, one of them being saturable with micromolar analyte concentrations, which is in agreement with previously determined K_D values ranging from 3 to 7 μM.[7,10]

FBP-Binding Induces the Disruption of Protein/Protein Interactions Involved in CggR/DNA Complex. In a previously published study, formation of the complex between CggR and its full-length DNA operator was investigated by analytical ultracentrifugation, revealing a 4:1 protein/DNA binding stoichiometry.[9] Additionally, it was demonstrated that at micromolar concentrations, FBP binding abolishes the binding cooperativity of CggR to its target DNA without altering the binding stoichiometry of the complex, suggesting a possible sugar-induced disruption of intermolecular protein/protein interactions within the CggR/DNA complex. In order to examine this hypothesis, we performed nanoESI-MS experiments with CggR in complex with either the full-length DNA operator (O_{LR}) or the right half-site operator (O_R) which displays a better affinity for CggR than the left one.[9] Briefly, as the binding stoichiometry of CggR to O_{LR} remains the same upon FBP binding, noncovalent MS would remain blind to putative disruption of protein/protein interactions (Figure 2a). On the contrary, with independent half-site operators, FBP binding is expected to affect CggR/O_R binding stoichiometry which could be monitored by nanoESI-MS (Figure 2b).

Accordingly, both complexes were first formed *in vitro*, purified by size-exclusion chromatography (see Experimental Section), and subsequently analyzed by noncovalent nanoESI-MS to determine their binding stoichiometries. The nanoESI mass spectrum obtained for the complex involving the full-length operator (Figure 3a) reveals the presence of a unique species with a measured

(49) Sugadev, R.; Balasundaresan, D.; Ponnuswamy, M. N.; Kumaran, D.; Swaminathan, S.; Sekar, K., to be submitted for publication.

(50) Smith, R. D.; Light-Wahl, K. J. *Biol. Mass Spectrom.* **1993**, *22*, 493–501.

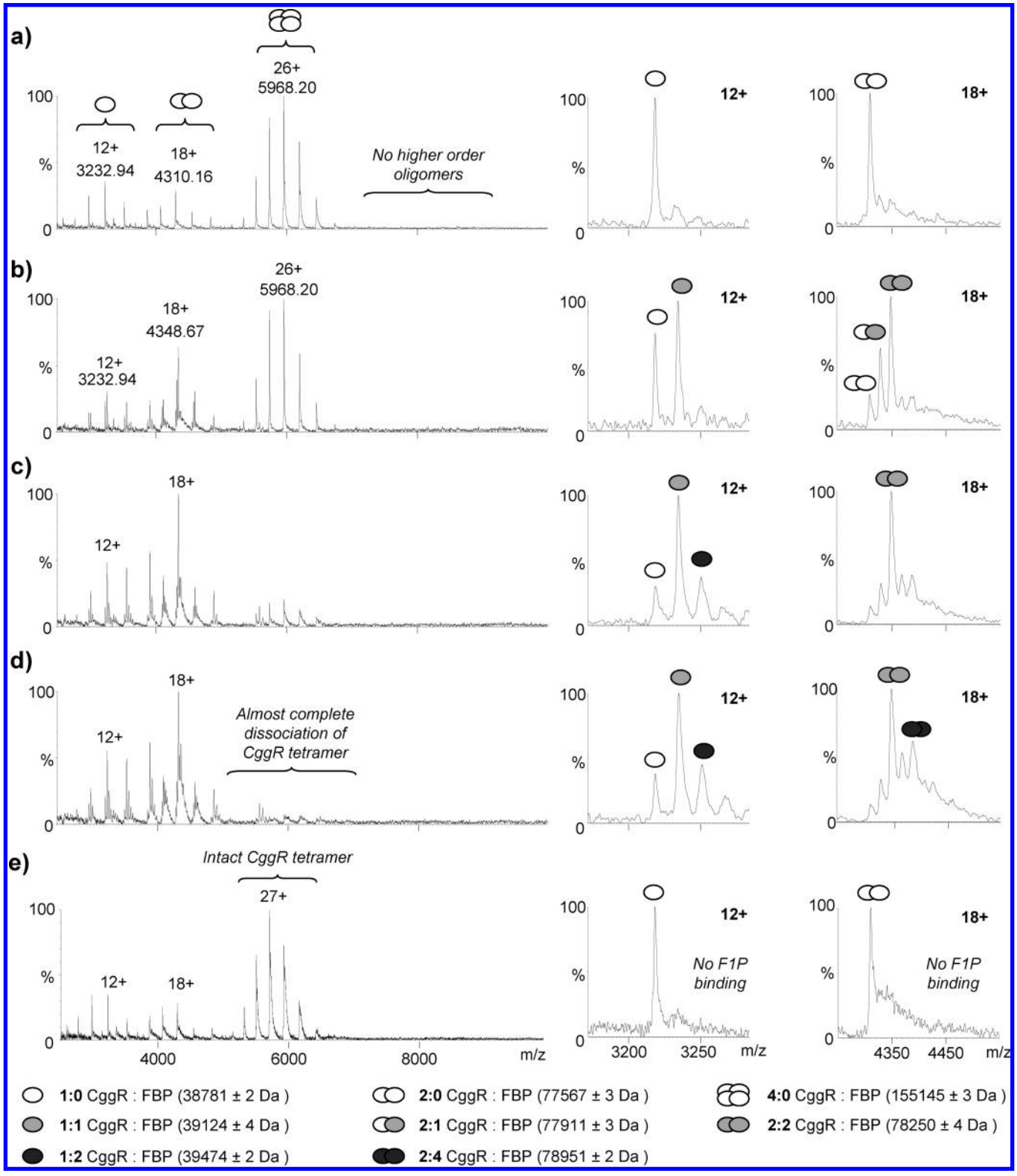

Figure 1. NanoESI-MS monitoring of FBP binding to CggR. CggR was diluted to 20 μM (monomer concentration) and analyzed either (a) alone or in presence of (b) 10 μM FBP, (c) 20 μM FBP, (d) 30 μM FBP, and (e) 30 μM F1P. Enlarged mass spectra from the right-hand columns correspond to the +12 charge state of monomeric CggR (2nd column) and the +18 charge state of dimeric CggR (3rd column). Vc = 120 V, Pi = 6 mbar.

molecular weight (182868 ± 9 Da) corresponding to a 4:1 CggR/O_{LR} complex (182802 Da). In the case of the complex formed with the right half-site operator O_R (Figure 3f), the most intense species is detected in the mass range m/z 7000−9000 with a molecular weight of 183 356 ± 5 Da corresponding to the 4:2 CggR/O_R complex (183298 Da). An additional minor ion distribution assigned to the 2:1 CggR/O_R complex (91649 Da) is also detected in the mass range m/z 4000−6000 with a measured molecular weight of 91 664 ± 5 Da. It is noteworthy that quasi-quantitative formation of the 4:2 CggR/O_R complex

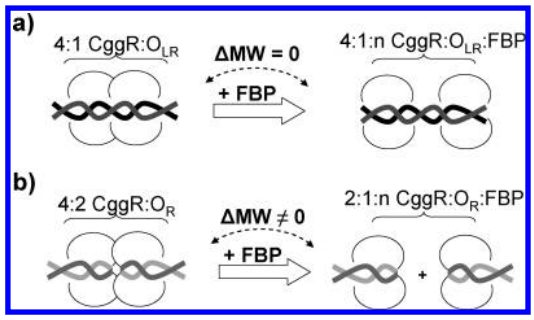

Figure 2. Working hypothesis used to enlighten FBP-induced disruption of protein/protein interactions within CggR/DNA complex. Upon FBP-induced disruption of protein/protein interactions, (a) the molecular weight of the 4:1 CggR/O_{LR} complex remains constant (ΔMW = 0 Da), while (b) the 4:2 CggR/O_R complex dissociation can be evidenced through mass measurements under nondenaturing conditions.

(instead of independent 2:1 CggR/O_R complexes) provides direct evidence for the existence of strong intermolecular protein/protein interactions within the CggR/DNA complex. In previously published work, this information about CggR/DNA complex architecture could only be indirectly inferred from correlation between the protein tetrameric oligomerization state and the 4:1 protein/full-length DNA binding stoichiometry.[9]

Next, titration experiments were carried out by incubating CggR/DNA complexes (3 μM) in the presence of increasing FBP concentrations. In the case of the complex formed with the full-length operator, the 4:1 CggR/O_{LR} complex remains almost completely intact upon FBP addition (Figure 3a−d). Indeed, although the 4:1 CggR/O_{LR} complex mainly binds three or four FBP molecules in the presence of a 10-fold molar excess of this effector sugar (30 μM, Figure 3d), only a small fraction of the 2:1 CggR/O_{LR} complex is observed. This observation is consistent with previous fluorescence anisotropy and electrophoretic mobility shift assay experiments showing that even millimolar concentrations of FBP do not allow a complete release of CggR from the complex.[9,10] Importantly, the nanoESI mass spectrum obtained under identical experimental and instrumental settings in the presence of F1P (30 μM, Figure 3e), the negative control sugar, only shows a single F1P adduct on the 4:1 CggR/O_{LR} complex. Such marked difference between both phosphorylated sugars indicates that FBP binding to 4:1 CggR/O_{LR} complex is mainly specific and does not merely result from nonspecific ligand adduction in solution and/or during the nanoESI process.[50]

In the case of the half-site operator, incubation of the 4:2 CggR/O_R complex (3 μM) with 1 mol equiv of FBP (3 μM) is sufficient to induce its partial dissociation into two 2:1 CggR/O_R complexes (Figure 3g). Complete dissociation is observed in the presence of 5 molar equivalents (15 μM) of effector sugar (Figure 3h), whereas even a 10-fold molar excess of negative control sugar (30 μM F1P, Figure 3j) is not able to provoke any significant complex dissociation. These results unambiguously demonstrate the ability of FBP to specifically induce the disruption of protein/protein interactions ensuring the integrity of the 4:2 CggR/O_R complex.

Interestingly, nanoESI mass spectra obtained for the complex formed with the half-site operator (Figure 3f−i) show that increasing FBP concentration leads first to complex saturation with a single FBP molecule per CggR subunit (detection of 2:1:2 CggR/O_R/FBP complex), as expected from the presence of a micromolar binding site on the protein.[7,10] Then, in the presence of 30 μM FBP (Figure 3i), complexes containing a second FBP molecule per CggR subunit are also observed (detection of 2:1:3 and 2:1:4 CggR/O_R/FBP complexes). Since the control experiment shows that only a single F1P adduct can be detected under strictly identical conditions (Figure 3j), it can be concluded that 2:1:3 and 2:1:4 CggR/O_R/FBP complexes are mainly specific, confirming again the presence of a second FBP binding site per CggR subunit.

Finally, it is noteworthy that the rate of FBP binding seems to be slightly higher in the case of CggR/O_R complex rather than CggR/O_{LR} complex (compare panels c and h in Figure 3). One should keep in mind that CggR/O_R complex is not a biologically relevant complex and has only been engineered in the present study to understand FBP-binding effect on CggR/DNA interactions. As a consequence, small differences can occur between both assemblies, as for example, a slightly different flexibility modifying the accessibility of FBP binding sites which could account for the differences observed in the number of FBP molecules bound to CggR/DNA complexes (compare panels c versus h in Figure 3). Thus, this comparison between both CggR/DNA constructs is purely qualitative and only intends to show that 4:1 CggR/O_{LR} complex remains intact upon FBP binding while 4:2 CggR/O_R dissociates into 2:1 CggR/O_R complex.

NanoESI-IM-MS Experiments Evidence CggR/DNA Conformational Changes upon FBP Binding. Above-described results clearly demonstrate that FBP specifically triggers the disruption of protein/protein interactions within CggR tetramer as well as 4:2 CggR/O_R complex. Extrapolating such observations to the 4:1 CggR/O_{LR} complex implies that significant conformational changes must occur upon FBP binding. Indeed, the strongest hint for such modifications arises from the outcomes of fluorescence-based techniques, suggesting that sugar binding increases the conformational dynamics of the CggR/O_{LR} complex.[9] In noncovalent MS, modifications of the tridimensional structure of biomolecules can be detected by a shift in the charge state distribution: the more extended the structure, the higher the number of charges carried by proteins.[51] In the present titration experiments, increasing FBP concentration only provokes a small shift of the 4:1 CggR/O_{LR} complex charge state distribution whose mean value increases from 22.6 in the absence of FBP (Figure 3a) to 23.8 in the presence of 30 μM FBP (Figure 3d), suggesting a slightly extended conformation of the complex in the presence of sugar. In order to obtain deeper insights into this conformational transition, nanoESI-IM-MS experiments were performed with CggR/O_{LR} complex, both in the absence and presence of FBP.

Collision Cross Section of CggR/DNA Assembly Increases upon FBP Binding. In order to investigate the effect of FBP binding on the conformation of CggR/DNA assembly, the 4:1 CggR/O_{LR} complex was first incubated at 3 μM in the absence of FBP. Subsequent nanoESI-IM-MS analysis shows that the +24 to +27 charge states of the complex are detected with drift times

(51) Chowdhury, S. K.; Katta, V.; Chait, B. T. *J. Am. Chem. Soc.* **1990**, *112*, 9012–9013.

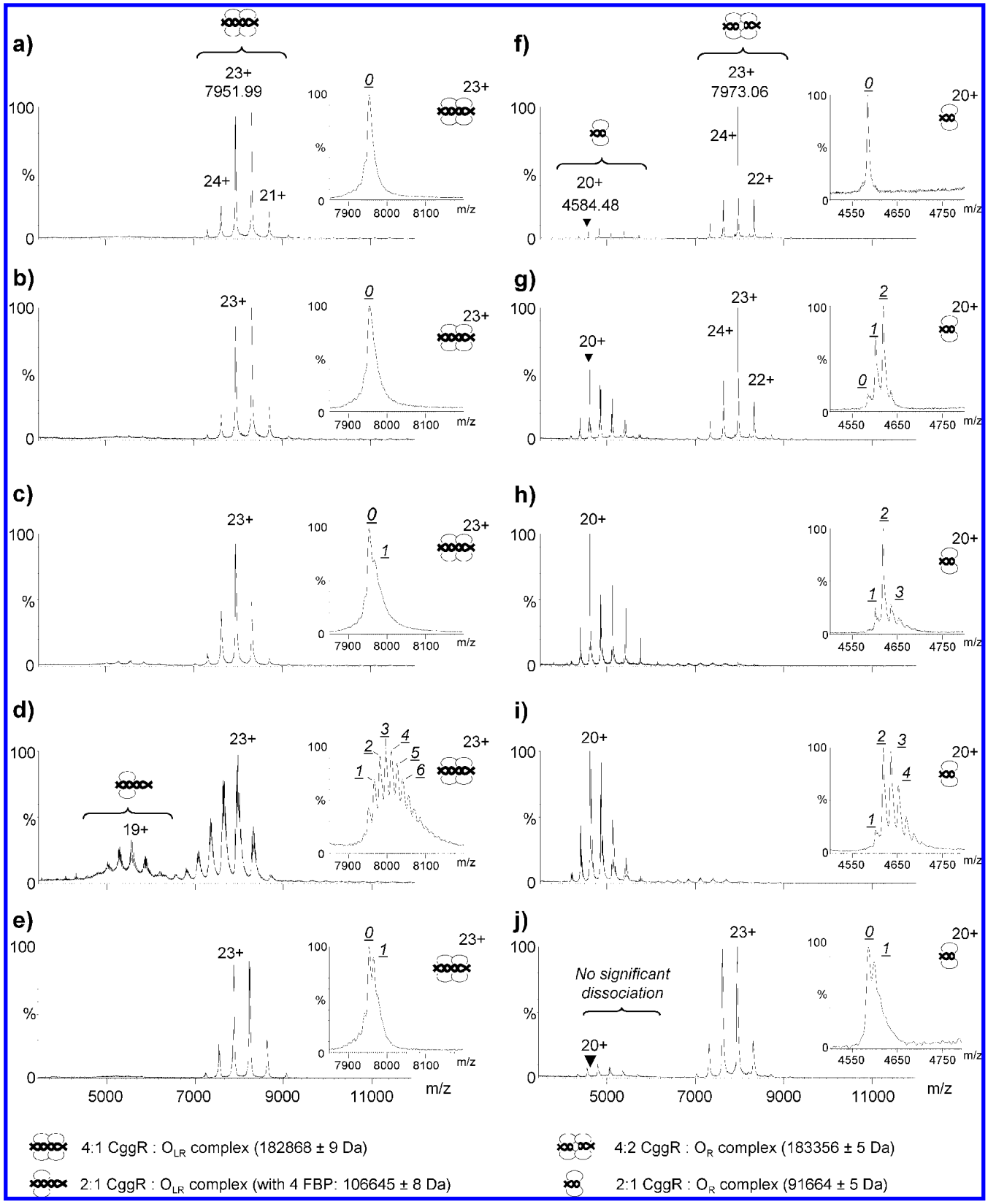

Figure 3. NanoESI-MS monitoring of FBP-binding effect on CggR/DNA complex. (a−e) CggR/O_{LR} complex and (f−j) CggR/O_R complex were diluted to 3 μM either (a, f) alone or in the presence of (b, g) 3 μM FBP, (c, h) 15 μM FBP, (d, i) 30 μM FBP, and (e, j) 30 μM F1P. Insets represent enlarged mass spectra showing (a−e) the +23 charge state of the 4:1 CggR/O_{LR} complex and (f−j) the +20 charge state of the 2:1 CggR/O_R complex. Underlined numbers correspond to the number of sugar molecules bound to each complex. Vc = 200 V, Pi = 7 mbar.

ranging from 8 to 16 ms (Figure 4a). Those drift times were corrected for the charge and reduced mass of the corresponding ion, so that CCS of each ion could be estimated using the calibration curve obtained with reference proteins (see Experimental Section). Averaging the CCS of 4:1 CggR/O_{LR} complex over the four most intense charge states (+24 to +27) yields

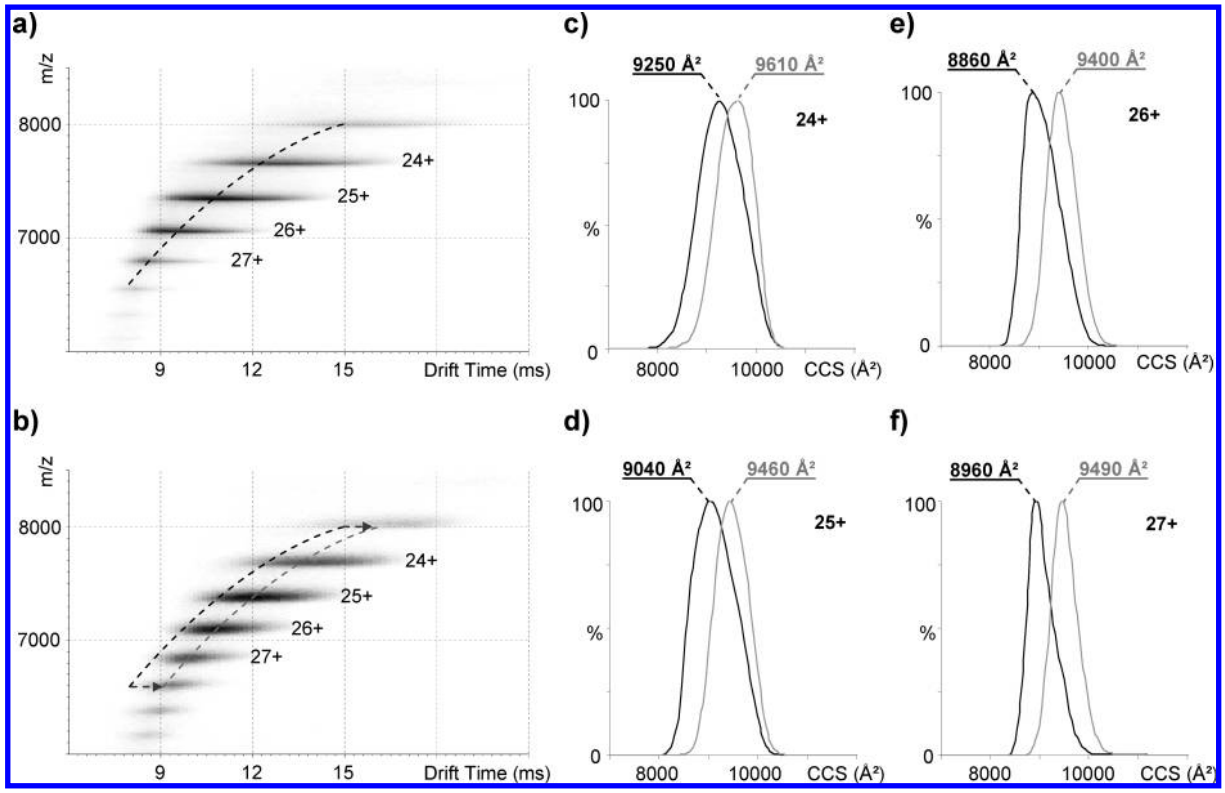

Figure 4. NanoESI-IM-MS monitoring of FBP-induced conformational modifications of CggR/O_{LR} complex. (a, b) Driftscopes were obtained for 4:1 CggR/O_{LR} complex diluted to 3 μM either (a) alone or (b) in the presence of 30 μM FBP. Arrival time distribution maxima of the most intense charge states are linked together by dashed curves. (c−f) CCS estimation for the +24 to +27 charge states of free and FBP-bound 4:1 CggR/O_{LR} complex. Black and gray curves are related to free and FBP-bound 4:1 CggR/O_{LR} complex, respectively.

a value of 9030 ± 165 Å^2 (Figure 4c−f). In contrast, when the 4:1 CggR/O_{LR} complex is incubated with a 10-fold molar excess of FBP (30 μM), the driftscope obtained under identical experimental and instrumental conditions reveals a significant shift in the measured drift times (Figure 4b). As gentle instrumental conditions required for CCS measurements (see Supporting Information S1) prevent the different FBP binding stoichiometries to be resolved, CCS were calculated over the different FBP ligation states (3 to 4 FBP molecules per 4:1 CggR/O_{LR} complex according to nanoESI-MS experiments, see above), leading to a CCS value (averaged over the +24 to +27 charge states) of 9490 ± 90 Å^2 for the FBP-bound form of 4:1 CggR/O_{LR} complex. Together with nanoESI-MS results obtained with CggR alone and in complex with the right half-site operator, this 5% increase of the CCS upon FBP binding provides strong evidence that this sugar is indeed able to trigger significant conformational alterations of the 4:1 CggR/O_{LR} complex by disrupting intermolecular protein/protein interactions without changing the complex binding stoichiometry.

Comparison with Solution-Based Techniques. Although a growing number of articles have demonstrated that gas-phase collision cross sections are in good agreement with values derived from other biophysical techniques,[37,40–42] the question of whether a protein or a complex can preserve its native conformation in a solvent-free environment remains a matter of debate.[52,53] In such a context, it is of interest to compare the results from nanoESI-IM-MS with those obtained by small-angle X-ray scattering (SAXS) and size-exclusion chromatography (SEC) experiments which were performed concomitantly to the present study.[47] SAXS can provide both the radius of gyration (R_g) and the molecular envelope of the analyte of interest, as well as estimations of its 3D structure based on rigid-body modeling. Regarding SEC, calibration with well-adapted standards allows determination of the Stokes radius (R_S). Table 1 summarizes the outcomes of these different techniques. While the relationship between R_g and R_S depends on the molecular shape of the analyte, both physical quantities are sensitive to the global shape and size of the molecule in solution. For the comparison of IM-MS results with these solution-based techniques, the radius ($R_{IM\text{-}MS}$) of free and FBP-bound 4:1 CggR complex was derived from the corresponding CCS assuming a spherical shape of the complex. $R_{IM\text{-}MS}$ is in good agreement with both R_g and R_S indicating that the 4:1 CggR/O_{LR} complex preserves a folded native-like conformation in the gas phase and that conformational modifications occurring in solution are at least partially conserved in this solvent-free environment. Table 1 also shows the CCS measured by nanoESI-IM-MS experiments compared to CCS estimations based on the molecular weight of the corresponding complexes. Those estimations were performed with a relationship relating the molecular weight to the CCS of roughly spherical ions.[38] Interestingly, significant differences are observed between measured and estimated CCS. This strongly suggests that the 4:1 CggR/O_{LR} complex has a nonspherical shape, consistent with the presence of a DNA framework which imposes a rather elongated shape to this assembly.[47]

(52) Meyer, T.; de la Cruz, X.; Orozco, M. *Structure* **2009**, *17*, 88–95.
(53) Breuker, K.; McLafferty, F. W. *Proc. Natl. Acad. Sci. U.S.A.* **2008**, *105*, 18145–18152.

Table 1. Comparison of IM-MS, SEC, and SAXS Experiments Performed on CggR/O_{LR} Complex in Absence and Presence of FBP[a]

technique	physical quantity	no FBP	+ FBP
IM-MS	$R_{IM\text{-}MS}$(nm)[b]	5.36 ± 0.05	5.50 ± 0.03
SEC	R_S(nm)	5.4 ± 0.2	5.8 ± 0.2
SAXS	R_g (nm)	4.46 ± 0.16	5.38 ± 0.11
IM-MS	measured MW (Da)	183131 ± 23	184207 ± 32[d]
	MW-based estimation of CCS (Å^2)[c]	7852	7883
	measured CCS (Å^2)	9030 ± 165	9490 ± 89[d]
SAXS	CCS from MOBCAL (Å^2)[e]	11160	11770

[a] SEC and SAXS data were obtained from Chaix et al.[47] [b] $R_{IM\text{-}MS} = (CCS/\pi)^{1/2}$. [c] $CCS = 2.435 \times MW^{2/3}$ according to Ruotolo et al.[38] [d] Mean value measured over the different FBP adducts. [e] SAXS-derived 3D models were used for CCS estimation using the EHSS method from MOBCAL.[47]

Finally, CCS values were estimated using MOBCAL and the atomic structure of the 4:1 CggR/O_{LR} complex obtained by rigid-body modeling and fitting to SAXS data.[47] While these MOBCAL estimations are somewhat higher than the corresponding IM-MS values, the calculated CCS values display a 5% difference between the free and FBP-bound forms of the complex, in agreement with the 5% increase measured in the gas phase. Consequently, the comparison with SEC and SAXS validates the present nanoESI-IM-MS results, showing that the CggR/DNA complex retains a memory of its solution structure in the gas phase and illustrating the potential of this technique to probe changes in the size and shape of proteins and noncovalent complexes in solution.

CONCLUSION

In the present study, we report the use of recent MS-based technologies to obtain detailed structural information on FBP-modulated CggR/DNA interactions. Using the 4:2 CggR/O_R complex, where both half-site operators are not covalently bound, we demonstrated that FBP binding leads to the symmetrical dissociation of this assembly into 2:1 CggR/O_R complexes. In contrast, the 4:1 CggR/O_{LR} assembly remains almost completely intact in the presence of FBP, most probably because full-length DNA acts as a framework holding the different protein subunits together in the complex. However, nanoESI-IM-MS experiments shed light on important FBP-induced changes in the structure of the 4:1 CggR/O_{LR} complex, as evidenced by the 5% increase of the complex CCS upon FBP binding. Notably, both the symmetrical dissociation and the increase of the complex CCS triggered by FBP binding corroborate a previously proposed model which suggests that CggR binds primarily as a dimer to each half-site of the full-length operator and that both dimers interact subsequently together, resulting in a cooperative protein binding to the DNA target which is abolished in the presence of FBP.[9] Taken together, the present results deepen our understanding of the mechanisms governing CggR interactions with its DNA target. Such knowledge is of crucial importance to decipher the underlying sugar-dependent transcriptional activation of glycolytic genes in *B. subtilis*.

The present study is also the first describing the use of nanoESI-IM-MS to detect ligand-induced conformational changes of a protein/DNA assembly. This article reports an interesting comparison between those gas-phase measurements and the data obtained by solution-based techniques. The close correlation found between the results from nanoESI-IM-MS, SAXS, and SEC indicates that CCS measurements in the gas phase can provide reliable information on the shape/size of native proteins and noncovalent complexes in solution. Finally, it is of interest to point out that nanoESI-IM-MS displays some unique advantages over biophysical techniques which are conventionally used for structural characterization of macromolecular complexes. Indeed, combining the MS dimension with ion mobility separation affords a simultaneous and independent determination of the binding stoichiometry and the CCS of noncovalent assemblies. Moreover, this technique does not require data modeling since it allows a direct and independent visualization of all ionizable species present in solution, as illustrated here through the simultaneous detection of protein/protein, protein/ligand, protein/DNA, and protein/DNA/ligand complexes. Those features of nanoESI-IM-MS, and more generally of noncovalent MS, make it a well-suited technique to investigate heterogeneous and poorly characterized systems where assumptions required by other techniques for data interpretation can hardly be justified.

ACKNOWLEDGMENT

This work was funded by the CNRS, the University of Strasbourg UdS, and the region Alsace. We thank the Fondation pour la Recherche Médicale for financial support of a Synapt HDMS mass spectrometer. C.A. and D.C. were supported by a studentship from the French Ministère de la Recherche. Authors would like to acknowledge Cyril Colas for FBP quantification and Cathy Royer for critical reading of the manuscript.

SUPPORTING INFORMATION AVAILABLE

Additional information as noted in text. This material is available free of charge via the Internet at http://pubs.acs.org.

Received for review December 8, 2009. Accepted March 8, 2010.

AC902784N